Aerosol Science and Technology
Publication details, including instructions for authors and subscription information:
http://www.informaworld.com/smpp/title~content=t713656376

Development of a Size-Selective Inlet-Simulating ICRP Lung Deposition Fraction

Yu-Mei Kuo [a]; Sheng-Hsiu Huang [a]; Tung-Sheng Shih [a]; Chih-Chieh Chen [a]; Yi-Mei Weng [a]; Wane-Yun Lin [a]
[a] Yu-Mei Kuo Sheng-Hsiu Huang Tung-Sheng Shih Chih-Chieh Chen Yi-Mei Weng Wane-Yun Lin Department of Occupational Safety and Health, Chung Hwa College of Medical Technology, Tainan, Taiwan Institute of Occupational Safety and Health, Council of Labor Affairs, Taipei, Taiwan Institute of Occupational Medicine and Industrial Hygiene, College of Public Health, National Taiwan University, Taipei, Taiwan .

First Published on: 05 July 2005

To cite this Article Kuo, Yu-Mei, Huang, Sheng-Hsiu, Shih, Tung-Sheng, Chen, Chih-Chieh, Weng, Yi-Mei and Lin, Wane-Yun(2005)'Development of a Size-Selective Inlet-Simulating ICRP Lung Deposition Fraction',Aerosol Science and Technology,39:5,437 — 443
To link to this Article: DOI: 10.1080/027868290956602
URL: http://dx.doi.org/10.1080/027868290956602

Aerosol Science and Technology, 39:437–443, 2005

ISSN: 0278-6826 print / 1521-7388 online
DOI: 10.1080/027868290956602

Development of a Size-Selective Inlet-Simulating ICRP Lung Deposition Fraction

Yu-Mei Kuo,[1] Sheng-Hsiu Huang,[2] Tung-Sheng Shih,[2] Chih-Chieh Chen,[3] Yi-Mei Weng,[3] and Wane-Yun Lin[3]

[1]*Department of Occupational Safety and Health, Chung Hwa College of Medical Technology, Tainan, Taiwan*
[2]*Institute of Occupational Safety and Health, Council of Labor Affairs, Taipei, Taiwan*
[3]*Institute of Occupational Medicine and Industrial Hygiene, College of Public Health, National Taiwan University, Taipei, Taiwan*

A size-selective inlet made of polyurethane filter foam was designed and fabricated to simulate a portion of the ICRP respiratory deposition curve. A downstream aerosol measuring device then could be used to generate aerosol concentration data that represented the fraction reaching the respiratory system. This article introduces useful knowledge about porous foam penetration for particle size ranges below those reported in the previous studies.

Different porosities of polyurethane foam filters were tested for aerosol penetration. Among the parameters operated in this work were (1) foam porosity (ppi), (2) filter thickness, (3) face velocity, and (4) packing density of the filter foams. Di-octyl phthalate was used as the test agent. A constant output atomizer and an ultrasonic atomizing nozzle were used to generate polydisperse submicrometer- and micrometer-sized particles, respectively. Aerosol concentrations and size distributions upstream and downstream of the filter foams were monitored by using a scanning mobility particle sizer (for particles with diameters smaller than 0.7 μm) and an aerodynamic particle sizer (for particles larger than 0.7 μm). The aerosol output was neutralized by a radioactive source. A lognormal-distribution curve with a mode of 0.25 μm and a GSD of 6.2 was set as the primary target curve simulating the light-work ICRP deposition model.

The results showed that the most penetrating size (also referred to as collection minimum) of the filter foams decreased upon increasing the foam porosity, packing density, and face velocity. In this work, the highest foam porosity and packing density we could acquire were 100 ppi and 0.2, respectively. By adjusting the face velocity, the most penetrating size was moved to 0.25 μm, which happened to be the most penetrating size for ICRP light-work criterion. The whole aerosol penetration curve could further fit to the modified ICRP curve by adjusting the filter thickness. There are numerous ways to match the ICRP definition. This size-selective inlet becomes even more versatile if the auxiliary detector and vacuum system are operated under different flow rates to simulate light-to-heavy workloads.

Received 4 January 2004; accepted 22 March 2005.
The authors would like to thank the Institute of Occupational Safety and Health, Council of Labor Affairs, Taiwan for the financial support through Grant No. IOSH-91-A104.
Address correspondence to Chih-Chieh Chen, Institute of Occupational Medicine and Industrial Hygiene, College of Public Health, National Taiwan University, 1 Jen-Ai Road, Sec. 1, Rm. 1440, Taipei, 10000, Taiwan. E-mail: ccchen@ntu.edu.tw

INTRODUCTION

The particle size distributions may be expressed in terms of either mass (volume), surface area, or number. Coarse aerosols (>1 μm) tend to dominate the size distribution, and perhaps health effects when the particle amount is specified in terms of particulate mass, but submicron aerosols (<1 μm) are more important when the particle number is of concern. For some fine aerosols, particle surface area is considered to be important, but current environmental regulations are mostly based on mass, because particle mass concentration remains the most likely metric for some other fractions and health effects (e.g., the respirable fraction and diseases like pneumoconiosis). Under normal atmospheric conditions, measured submicrometer-sized aerosol concentration in terms of mass is lower than the coarse aerosol. However, evidence shows that the aerosol number concentration might be a more sensitive indicator than aerosol mass concentration because aerosol number concentration can present a better correlation between exposure and disease (Oberdörster 2001), in particular for particles composed of low-toxicity and low-solubility materials (Donaldson et al. 2000). Furthermore, deposition is an essential step in establishing a physical link between the exposure measurement and the aerosol deposition on the lung surface as dose (Brand et al. 1997; Kim and Jaques 2000). Therefore, a size-selective aerosol sampler was developed in this work in order to provide a more accurate way to assess the health hazard of fine particulates.

Flexible polyurethane foams meet many design criteria for a variety of filtration functions, including demisting, humidification, and oil/water separation. The major benefits of filter foams are their relatively low air resistance and low pressure drop due

to the open-pore skeletal structure, large dust-holding capacity due to the 97% void volume, and design potential for easy installation and space savings due to the high tensile strength and tear resistance. There are many other benefits of using filter foams. Several semiempirical models for porous foam aerosol penetration have been developed (Wake and Brown 1991; Vincent et al. 1993; Brown 1993; Kenny et al. 2001). Filter foams have been used to match particle size fraction definitions for health-related sampling (Brown 1979; Courbon et al. 1988; Chung et al. 1997; Vincent et al. 1993; Chen et al. 1998), but mainly for particles larger than 1 μm.

In this project, the particle size range of interest was expanded to cover from nanometers to tens of micrometers. The filter foams were chosen to study the effect of packing density on the filtration characteristics because filter foams can be compressed to increase the packing density without changing the fiber diameter. The filter foams, used as a size-selective inlet, remove the large and small particles, and they produce an aerosol that simulates the fraction reaching the lung. Then a downstream aerosol-measuring device can be used to generate aerosol concentration data for more accurate exposure and risk assessment.

FILTRATION MECHANISMS

In general, air filtration is a complex process. Classical filtration theory begins with an isolated fiber, and the collection efficiency of a fiber is defined as the ratio of the inlet height of the limiting particle trajectory to the fiber diameter. The more modern single-fiber theory takes into account the effect of adjacent fibers. The theoretical aerosol penetration of a particle with n elementary charges, P_n, through a filter is normally expressed in terms of total single-fiber efficiency, $E_{\Sigma,n}$ (Hinds 1999),

$$P_n = \exp\left[\frac{-4\alpha\chi E_{\Sigma,n}}{\pi d_f(1-\alpha)}\right], \quad [1]$$

where α is packing density, χ is filter thickness, d_f is fiber diameter, and $E_{\Sigma,n}$ is given by (Lathrache and Fissan 1987; Tennal et al. 1991)

$$E_{\Sigma,n} = 1 - (1 - E_m)(1 - E_{e,n}). \quad [2]$$

In Equation (3), E_m is the total single-fiber efficiency due to the mechanical force, given as

$$E_m = 1 - (1 - E_{dr})(1 - E_i)(1 - E_g), \quad [3]$$

and $E_{e,n}$ is the total single-fiber efficiency due to the electrical force, given as

$$E_{e,n} = 1 - (1 - E_p)(1 - E_{c,n})(1 - E_{m,n}), \quad [4]$$

where E_{dr} is due to diffusion and interception (Lee and Liu 1982), E_i is due to impaction (Hinds 1999), E_g is due to gravitational settling (Hinds 1982), E_p is due to dielectrophoretic force, $E_{c,n}$ is due to the Coulombic force (Lathrache and Fissan 1987; Tennal et al. 1991), and $E_{m,n}$ is due to the image force (Kanaoka et al. 1987). The above equation is an approximation based on the assumptions that the electret filters have a uniform charge on their fibers and all individual filtration mechanisms are independent. It is assumed that the particle charges are in Boltzmann charge equilibrium and the interaction terms between the individual mechanisms are not within the scope of the present study. A spreadsheet (Microsoft Excel) was used to calculate and integrate the filtration efficiency by each individual filtration mechanism. The in-depth information of all individual filtration mechanisms has been summarized previously (Chen et al. 1993) and is not reiterated here.

EXPERIMENTAL MATERIALS AND METHODS

Di-octyl phthalate (DOP) was used as the test agent. In order to cover a broad size range, a constant output atomizer (model 3076, TSI Inc., St. Paul, MN, USA), and an ultrasonic atomizing nozzle (model 8700-120, Sonotek Inc., Highland, NY, USA), were used to generate polydisperse submicrometer- and micrometer-sized particles, respectively. The aerosol output was neutralized to Boltzmann charge equilibrium by a radioactive source, Po-210, and then introduced into the mixing and test chamber as shown in Figure 1. Two different particle size spectrometers were used to measure the aerosol concentrations and size distributions upstream and downstream of the filters: a scanning mobility particle sizer (SMPS, model 3934, TSI Inc.)

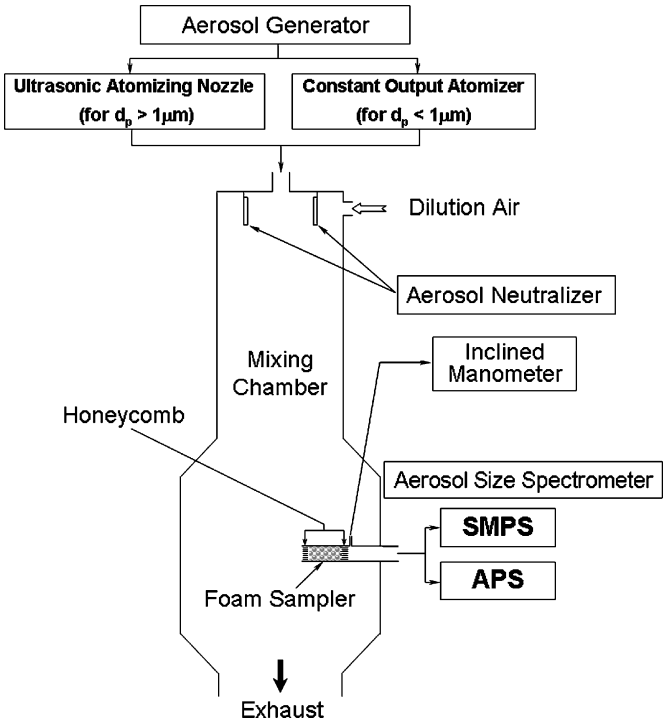

FIG. 1. The diagram of the experimental system setup.

for particles smaller than 0.7 μm, and an aerodynamic particle sizer (APS, model 3320, TSI Inc.) for particles larger than 0.7 μm. Since the density of DOP is close to unity, the size measured by using APS-3320 can also be regarded as physical diameter. Flexible polyurethane foams were selected for their relatively low pressure drop due to the open-pore skeletal structure and their low packing density (97% void volume). A punch was used to make foam pieces into the disc shape with a diameter of 18 mm, which were then inserted (with slight compression) into a holder with a diameter of 17 mm. The most important property of filter foams applied in this work is that the fiber diameter would not change when the foams were compressed to change the packing density (ratio of solid volume to total volume, also referred to as solidity). An inclined manometer was used to monitor the pressure drop across the filter foams. The honeycomb was used to compress the filter foams to increase the packing density. The honeycomb became distorted when the packing density exceeded 0.22.

The major operating parameters and their ranges were face velocity (1 $\sim$ 140 cm/s), packing density (0.08 $\sim$ 0.2), and fiber diameter (36, 47, 66, and 154 μm), or the corresponding nominal sizes (100, 80, 60, and 30 pores/in) as provided by the manufacturer (Fomax International Inc., Eddystone, PA, USA). Fiber diameter-to-pore-size conversion was based on the empirical relationship, $d_f = (0.009633\ (\text{porosity})^{-1.216})$, derived by Vincent et al. (1993). All air flows were controlled and monitored by mass flow controllers (Hastings Instruments, Hampton, VA, USA).

The light-work International Commission on Radiological Protection (ICRP) deposition model (ICRP 1994) was chosen as the target curve. After subtracting the sum of the fractional deposition efficiencies in the head, tracheobronchial tree, and nonciliated pulmonary regions, this penetration efficiency curve has the most penetrating size (MPS, also referred to as collection minimum), at 0.25 μm, for the light-exercise category of ICRP, as shown by the dashed line in Figure 2. The increase in aerosol penetration for particles larger than 10 μm is probably due to the decrease in inspirability. From the single-fiber theory, the calculated penetration curves are all bell-like. Empirically, a lognormal distribution curve was obtained by iteration, and the geometric standard deviation (GSD) of extent of the spread was found to be of 6.2.

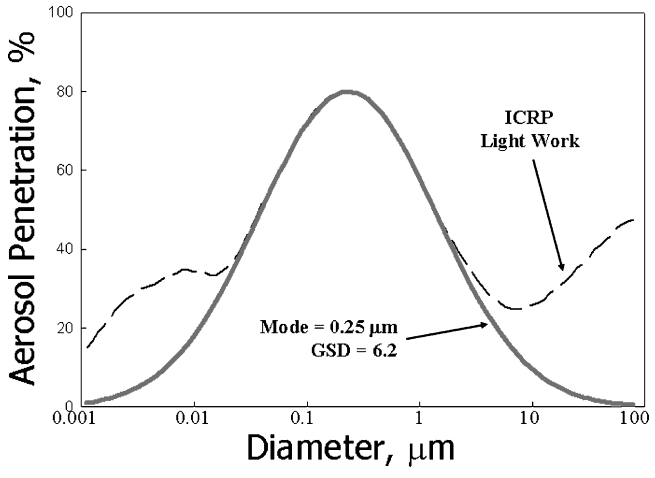

FIG. 2. A log-normal distribution curve corresponding to the ICRP light-work criterion.

RESULTS AND DISCUSSION

The effect of face velocity on aerosol penetration is shown in Figure 3. The solid thin line represents the target penetration curve. With the foam disk (60 ppi or $d_f = 66$ μm) compressed to have a packing density of 0.14 and thickness of 50 mm, the aerosol penetration, in particular for submicrometer-sized particles, increases with increasing face velocity, apparently due the shorter retention time in the filter media to deposit by diffusion. For micrometer-sized particles, the aerosol penetration might decrease with increasing face velocity due to stronger inertial impaction. The experimental data (upper plot) shows a similar trend with the modeled penetration curves (lower plot). Notice that at very high face velocity over 100 cm/s, the aerosol penetration for the size smaller than MPS stops increasing and instead begins to decrease, because even for aerosols smaller

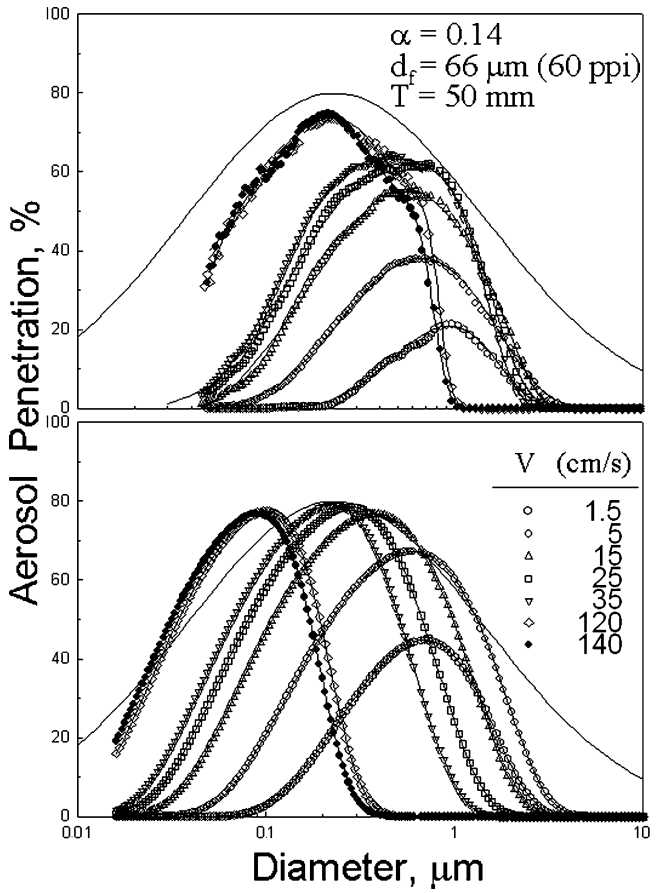

FIG. 3. Effect of face-velocity on aerosol penetration.

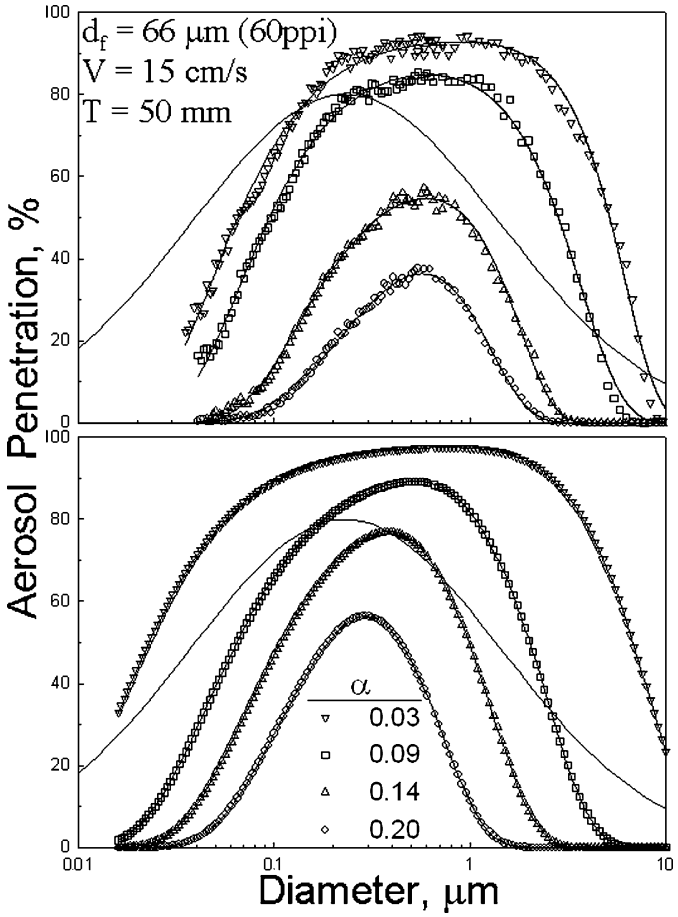

FIG. 4. Effect of packing density on aerosol penetration.

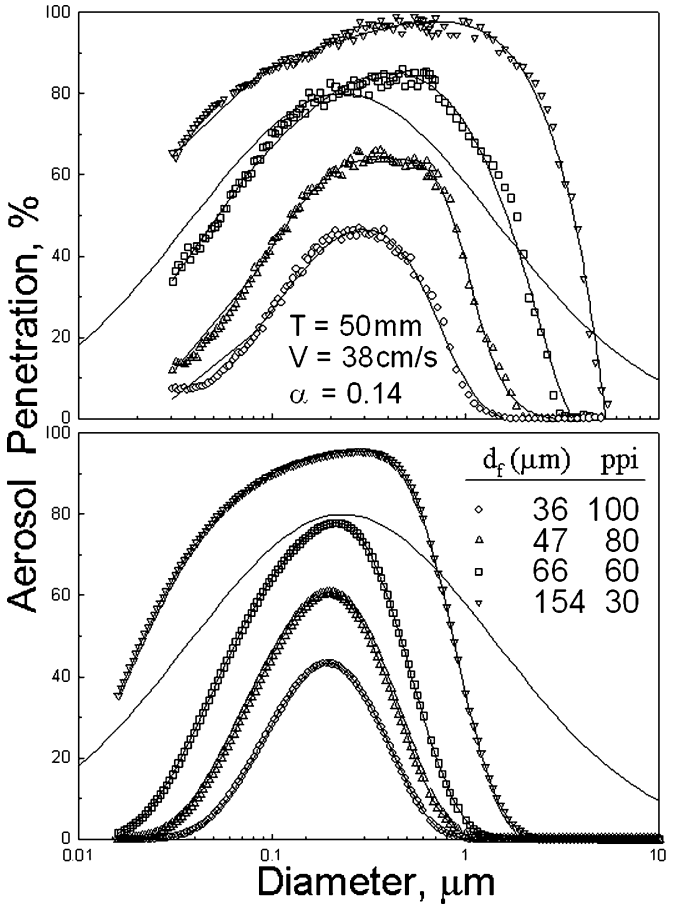

FIG. 5. Effect of fiber diameter (nominal size of foam) on aerosol penetration.

than 0.1 μm the inertial impaction exceeds the diffusion. In addition to the influence on aerosol penetration, the face velocity also plays an important role on the MPS. As shown in Figure 3, the MPS decreases with increasing face velocity much more significantly than other parameters, as will be discussed below.

The aerosol penetration decreases as the packing density increases, as shown in Figure 4, with filter foam of 60 ppi (66 μm) and thickness of 50 mm, under the face velocity of 15 cm/s. The shift of filtration mechanism may occur if the packing density is extremely high. However, in the present study, the decrease in aerosol penetration is mainly due to more filter materials, i.e., more surface area for aerosol particles to deposit on. The MPS decreases with increasing packing density but the size range (0.2 $\sim$ 0.7 μm) is not as wide as that influenced by the face velocity (0.08 $\sim$ 0.8 μm, according to the modeled penetration data).

Fiber diameter affects the aerosol penetration very much in the same way as the packing density but to an even lesser extent. Aerosol penetration through a disk of foam (thickness 50 mm, packing density 0.14, face velocity of 38 cm/s) decreases with decreasing fiber diameter, as shown in Figure 5. With the packing density fixed at 0.14, the surface area increases (proportional to the square of ratio of fiber diameter) due to the fact that the fiber diameter becomes smaller. The MPS also decreases with decreasing fiber diameter, albeit to a lesser extent than the packing density.

According to filtration theory, the filter thickness would not affect the most penetrating size. Therefore, the extent of the effects of other three parameters (face velocity, packing density, and fiber diameter) on the MPS is shown in Figure 6. The extreme values of these factors were used to demonstrate the range of their influence. Among the major parameters, face velocity affects the largest range of MPS, followed by packing density and then fiber diameter.

The search toward the ICRP light-work curve can be easier if the first piece of foam has a MPS close to 0.25 μm (MPS of ICRP), if not an exact match. From Figures 4, 5, and 6 we learn that high packing density (0.2) and small fiber diameter (36 μm/100 ppi) lead to a MPS that is slightly larger than 0.25. Therefore, the most-porous foam (100 ppi) was compressed to have a packing density of 0.22. The aerosol penetration curves

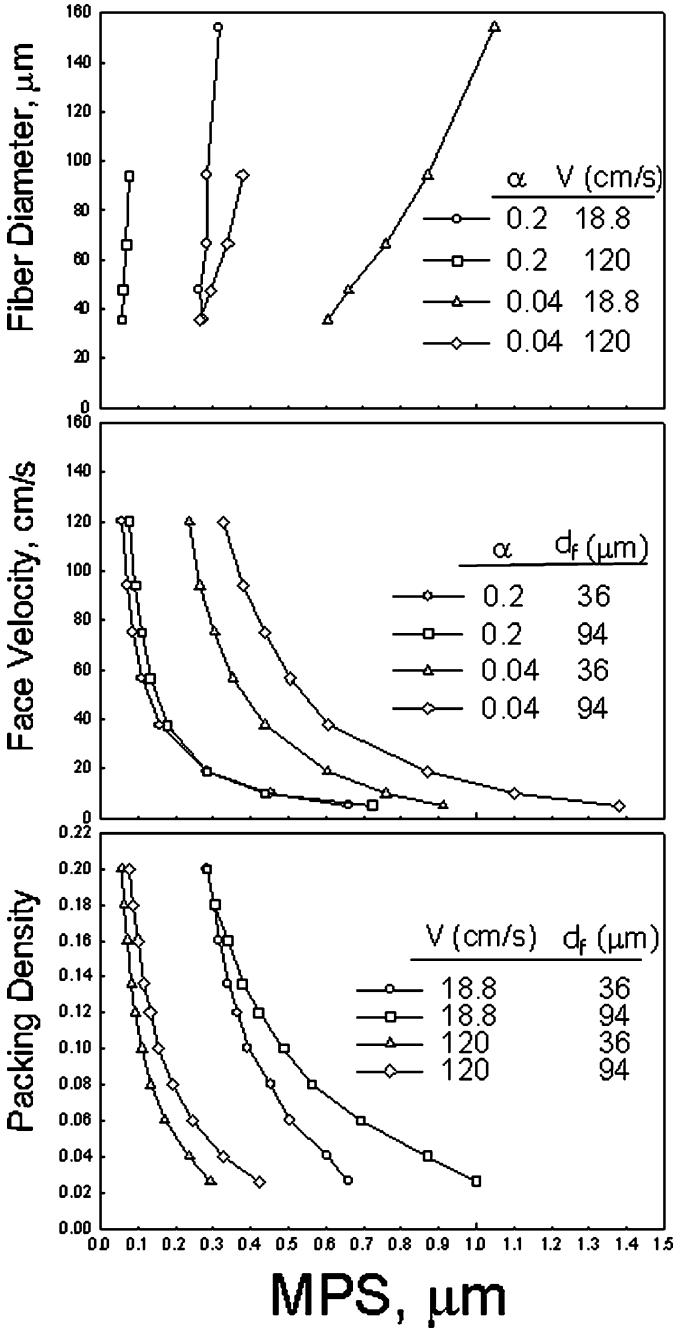

FIG. 6. Extent of effect of fiber diameter, face velocity, and packing density on the most-penetrating size.

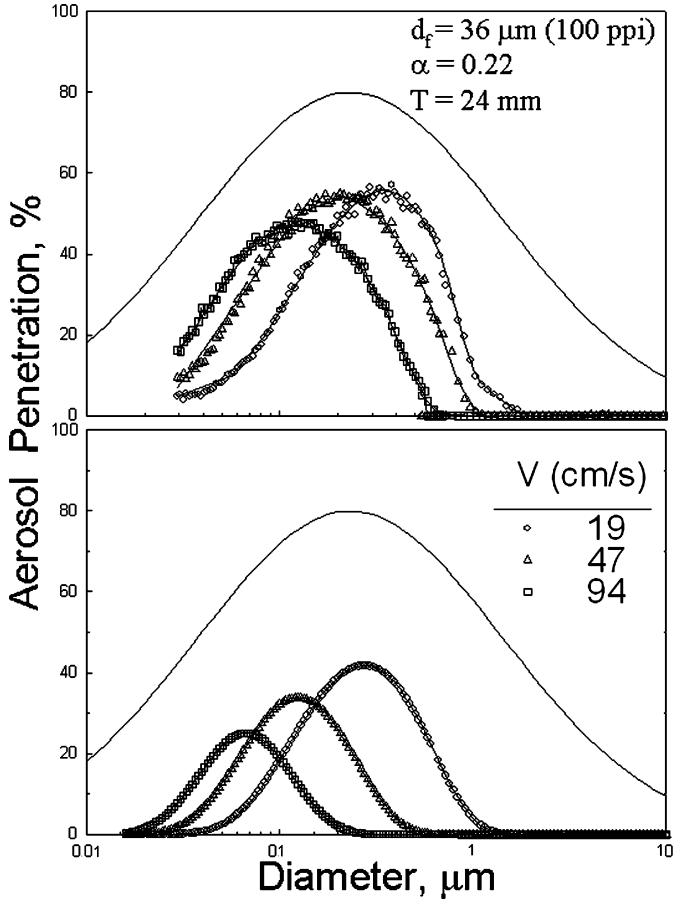

FIG. 7. The search for the most-penetrating size at 0.25 μm by adjusting the face velocity. The highest packing density of this work, 0.22, and the smallest fiber diameter were chosen because of the tendency of approaching the MPS.

move toward small particle size as the face velocity increases (from 19 to 94 cm/s), and they even surpass the target MPS of 0.25 μm. The most-penetrating size approached 0.25 μm when the face velocity was set at 47 cm/s, as shown in the top plot of Figure 7. In order to improve the fit to the ICRP curve, the next easy step is to simply decrease the filter thickness from 24 to 8 mm, as is shown in Figure 8. For particles larger than 1 μm, the foam penetration curve differs significantly from the ICRP criterion. However, this might be just a negligible flaw if the main use of this filter foam is for measuring the number of areosols deposited (or penetrated) in the respiratory tract, because the aerosol number concentration of micrometer-sized particles is normally lower than 10 #/cm^3, which is three magnitudes lower than that observed in normal atmospheric or indoor environments.

Because of the limitation on the foam solidity (0.03 $\sim$ 0.2) and nominal size (30 $\sim$ 100 ppi), how and to what extent these factors affect the spread of aerosol penetration were demonstrated using three combinations, as shown in Figure 9. All the three combinations have an MPS of 0.25 μm. Higher packing density (α = 0.2), smaller fiber diameter (d_f = 36 μm), and higher face velocity (94 cm/s) tend to have wider distributions.

The determination of the best combination of foam properties and operation conditions can be a very complex process. For

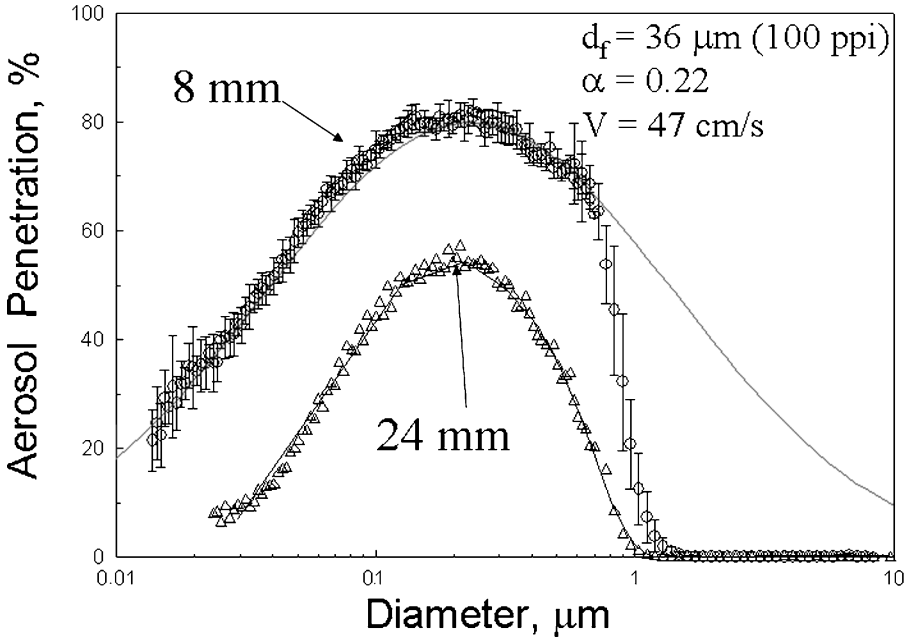

FIG. 8. Adjusting the foam thickness to match the near-ICRP curve.

industrial hygiene applications, the sampler needs to be handy and rugged and consume the least energy. Therefore, the filter quality factor and the sampling flow should also be taken into consideration. One of the advantages of using filter foams is that the sampling flow can be adjusted by changing the size of the holder while the face velocity remains unchanged. This size-selective sampler becomes even more versatile if the auxiliary detector and vacuum system are operated under different flow rates to simulate different workloads.

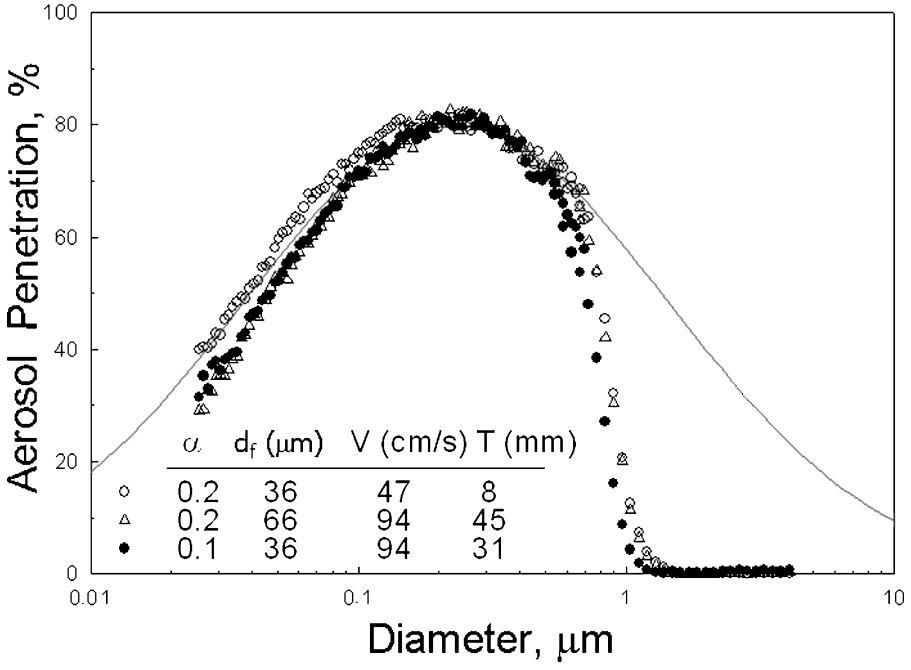

FIG. 9. Sample combinations of filter foams to be used as size-selective aerosol number sampler.

CONCLUSIONS AND RECOMMENDATIONS

The experimental data of aerosol penetration curves and derived MPS might not be exactly identical with the modeled values based on single-fiber theory because of the simplified nature of modeling. Yet, the models showed precisely the same trend with the experiments, an indispensable advantage of modeling. In fact, with the interaction among all individual filtration mechanisms remaining unsolved, and other oversimplified assumptions, the single-fiber theory is more than satisfactory when using as a tool to search for a size-selective aerosol sampler.

A log-normal distribution used to simulate the ICRP light-work criterion has a mode at about 0.25 μm and a GSD of 6.2. The aerosol penetration of the most-penetrating size was about 80%. If an aerosol size spectrometer was used to measure the aerosol concentration and size distribution, the correction for airway deposition–penetration can be performed mathematically. However, most of the aerosol size spectrometers are quite heavy and clumsy, and thus they are not suitable for personal sampling. Another problem with most aerosol size spectrometers is that they cover only a portion of the size range of interest. Therefore, a light and handy sensor, such as condensation nuclei counter, is ideal for assessing the health hazard of fine particles.

For aerosol particles (>1 μm) traveling fast (>15 cm/s), inertial impaction is the dominating filtration mechanism. Aerosol penetration decreases with increasing face velocity for particles <1 μm, indicating diffusion is the principal filtration mechanism. The MPS decreases with increasing face velocity, increasing packing density, and decreasing fiber diameter. Filter thickness does not affect the shape of the aerosol penetration curves.

In this work, the face velocity has the greatest influence on the range of the MPS, followed by packing density and then fiber diameter. As to the extent of the spread of aerosol penetration curve, higher packing density, lower face velocity, and smaller fiber diameter all lead to a wider distribution. According to theory, there should be numerous combinations of fiber diameter, packing density, and filtration velocity that have a satisfactory fit to the ICRP light-work curve.

REFERENCES

Brand, P., Rieger, C., Schulz, H., Beinert, T., and Heyder, J. (1997). Aerosol Bolus Disperse in Healthy Subjects, *Eur. Respir. J.* 10:460–467.

Brown, R. C. (1993). Air Filtration—*An Integrated Approach to the Theory and Applications of Fibrous Filter*. Oxford, Pergamon Press, pp. 21–23.

Brown, R. C. (1979). Porous Foam Size Selectors for Respirable Dust Sampler, *J. Aerosol Sci.* 11:151–159.

Chen, C. C., Lai, C. Y., Shih, T. S., and Yeh, W. Y. (1998). Development of Respirable Aerosol Samplers Using Porous Foams, *Am. Ind. Hyg. Associ. J.* 59:766–773.

Chen, C. C., Lehtimaki, M., and Willeke, K. (1993). Loading and Filtration Characteristics of Filtering Facepieces, *Am. Ind. Hyg. Assoc. J.* 54(2):51–60.

Chung, K. Y. K., Aitken, R. J., and Bradley, D. R. (1997). Development and Testing of a New Sampler for Welding Fume, *Ann. Occup. Hyg.* 3:355–372.

Courbon, P., Wrobel, R., and Fabries, J. F. (1988). A New Individual Respirable Dust Sampler: The CIP10, *Ann. Occupat. Hyg.* 32:129–143.

Donaldson, K., Stone, V., Gilmour, P. S., Brown, D. M., and Macnee, W. (2000). Ultrafine Particles: Mechanisms of Lung Injury. *Philos. Trans: Math. Phy. Eng. Sci.* 358(1775):2741–2749.

Hinds, W. C. (1999). *Aerosol Technology*. New York, John Wiley and Sons, Inc., pp. 182–205.

International Commission on Radiological Protection (ICRP). (1994). *Human Respiratory Tract Model for Radiological Protection*. ICRP publication 66. Ann. ICRP 24, Nos 1–3.

Kanaoka, C., Emi, H., Otani, Y., and Iiyama, T. (1987). Effect of Charging State of Particles on Electret Filtration, *Aerosol Sci. Technol.* 7:1–13.

Kenny, L. C., Aitken, R. J., Beaumont, G., and Görner, P. (2001). Investigation and Application of a Model for Porous Foam Aerosol Penetration, *J. Aerosol Sci.* 32:271–285.

Kim, C. S., and Jaques, P. A. (2000). Respiratory Dose of Inhaled Particles in Healthy Adults, *Philos. Trans. Math. Phys. Eng. Sci.* 358(1775):2693–2705.

Lathrache, R., and Fissan, H. J. (1987). Enhancement of Particle Deposition in Filters Due to Electrostatic Effects, *Filtration Separation* 24(6):418–422.

Lee, K. W., and Liu, B. Y. H. (1982). Theoretical Study of Aerosol Filtration by Fibrous Filter. *Aerosol Sci. Technol.* 1:147–161.

Oberdörster, G. (2001). Pulmonary Effects of Inhaled Ultrafine Particles. *Int. Arch. Occup. Environ. Health* 74:1–8.

Tennal, K. B., Mazumder, M. K., Siag, A., and Reddy, R. N. (1991). Effect of Loading with an Oil Aerosol on the Collection Efficiency of an Electret Filter, *Particulate Sci. Technol.* 9:19–29.

Vincent, J. H., Aitken, R. J., and Mark, D. (1993). Porous Plastic Foam Filtration Media: Penetration Characteristics and Applications in Particle Size-Selective Sampling, *J. Aerosol Sci.* 24(7):929–944.

Wake, D., and Brown, R. C. (1991). Filtration of Monodisperse Aerosols and Polydisperse Dusts by Porous Foam Filters. *J. Aerosol Sci.* 22(6):693–706.